(2)

NSWCDD/TR-92/303

REVERSE-BALLISTIC IMPACT STUDY OF SHEAR PLUG FORMATION AND DISPLACEMENT IN Ti6Al4V ALLOY

BY WILLIAM H. HOLT WILLIS MOCK, JR. WILLIAM G. SOPER
WEAPONS SYSTEMS DEPARTMENT

CHARLES S. COFFEY
RESEARCH AND TECHNOLOGY DEPARTMENT

JUNE 1992

NAVAL SURFACE WARFARE CENTER
DAHLGREN DIVISION
Dahlgren, Virginia 22448-5000

NSWCDD/TR-92/303

REVERSE-BALLISTIC IMPACT STUDY OF SHEAR PLUG FORMATION AND DISPLACEMENT IN Ti6Al4V ALLOY

BY WILLIAM H. HOLT WILLIS MOCK, JR.
WILLIAM G. SOPER
WEAPONS SYSTEMS DEPARTMENT

CHARLES S. COFFEY
RESEARCH AND TECHNOLOGY DEPARTMENT

JUNE 1992

NAVAL SURFACE WARFARE CENTER
DAHLGREN DIVISION
Dahlgren, Virginia 22448-5000

FOREWORD

The purpose of this basic research work was to obtain information on the energetics of shear plug formation and displacement in metals for validation of existing theories and to obtain information on the microstructural details associated with the shear plugging process.

A gas gun and precision impact configurations were used to provide control of the impact velocities and geometries to limit the variables in the experiments to the parameters of interest. The Ti6Al4V alloy was selected for this work because it is known experimentally to be very prone to adiabatic shear band formation in response to high strain rate loading.

The shear plugging experiments described in this report represent the first reported measurements of unconstrained incremental displacements of shear plugs through target plates. The dynamical model developed by W. G. Soper as part of this work relates shear plug displacements to the impact velocities and provides the first reported experimental determinations of (a) the threshold energy required to initiate shear plug displacement and of (b) the shear strength of the material within the main shear zone that defines the boundary of the plug. These experiments also provide clear evidence for material melting in the shear plugging process.

This work was performed as part of a Naval Surface Warfare Center Dahlgren Division (NSWCDD) Independent Research Project. This report has been reviewed by W. E. Hoye, Head, Warheads Branch and by D. L. Brunson, Head, Missile Systems Division.

The authors would like to acknowledge the assistance of P.J. Dudt of the Naval Surface Warfare Center Carderock Division in obtaining the Ti6A14V material. V. Ramachandran and R.W. Armstrong of the University of Maryland are acknowledged for helpful discussions. X.J. Zhang of the University of Maryland assisted in obtaining some of the optical and scanning electron micrographs. M.K. Norr of the Naval Surface Warfare Center Dahlgren Division provided the scanning electron micrograph of the melted materal on the separated shear plug.

Approved by:

David Malyevac

DAVID S. MALYEVAC, Deputy Head
Weapons Systems Department

ABSTRACT

Gas-gun reverse-ballistic experiments have been performed in which Ti6Al4V alloy disks were impacted onto smaller diameter, hardened steel rods to push out shear plugs from the disk material. The range of disk velocities was 219 to 456 m/sec. For each experiment, the disk, plug, and rod were soft recovered after impact. Below 290 m/sec, the plugs were pushed only part way through the disks, but localized shear bands outlining the plug shapes were easily recognized in metallographic sections. Optical and scanning electron microscopies were used to determine shear zone widths and to describe microstructural details associated with the primary shear zones. There is evidence for appreciable adiabatic heating and consequent thermal softening and melting of material in the main shear zone. A simple model is used to relate the observed plug displacements to the impact velocities and to provide estimates of several features: the shear zone strength, the threshold energy for shear plug displacement, and the threshold energy for shear plug separation. Clear evidence is presented of molten material having been produced as part of the plug separation process.

CONTENTS

ILLUSTRATIONS

ILLUSTRATIONS (Continued)

TABLE

I. INTRODUCTION

Adiabatic shear bands are narrow regions of localized deformation that can result from high strain rate loadings such as projectile impact and explosive forming operations. Timothy[1] has provided a recent critical review of shear band deformation in several metals. Titanium and titanium-based alloys are known to be shear band prone. Meyers and Pak[2] have studied impact-induced shear bands in commercially pure titanium by high-voltage transmission electron microscopy and scanning electron microscopy. Shear banding has been reported in microstructural studies of impacted plates of Ti6Al4V alloy by Woodward[3] and by Me-Bar and Shechtman.[4] Dormeval and Ansart[5] observed shear bands in Ti6Al4V alloy fractured in dynamic compression in a Hopkinson bar apparatus. This report is concerned with shear banding in reverse-ballistic impact experiments on Ti6Al4V alloy over a range of impact velocities. In each experiment, a disk of the alloy is accelerated in a gas gun and impacted onto an initially stationary, smaller diameter, hardened steel rod to push out a plug of disk material. The experiments include impact velocities where the plug is pushed only partway through the disk, as well as higher velocities where the plug is completely separated. The microstructural features of the shear bands and surfaces of separation are described. A preliminary report has been given of the work.[6]

II. IMPACT EXPERIMENTS

A 40-mm-bore gas gun[7] was used for the impact experiments. Figure 1 is a schematic of the gas gun. A sabot with a Ti6Al4V impactor disk is loaded into the barrel, and a target holder containing a hard steel rod is mounted on the muzzle of the gun. The barrel is evacuated to 0.1 Pa pressure to minimize gas cushion effects at impact. The breech pressure vessel is filled with nitrogen or helium gas to the desired pressure, and the gun is fired by actuating the fast-opening valve. The reverse-ballistic impact configuration (disk or plate impacting rod instead of vice versa) has the advantage of permitting precise control of the impact geometry. Figure 2 is an overview of the gas gun from the breech end.

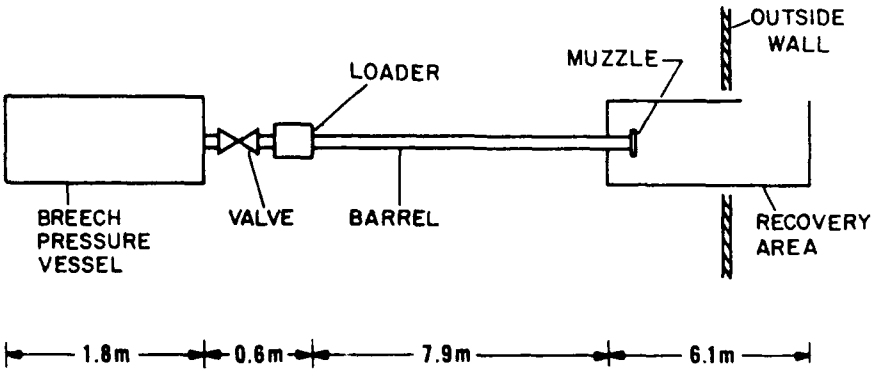

FIGURE 1. SCHEMATIC OF GAS GUN

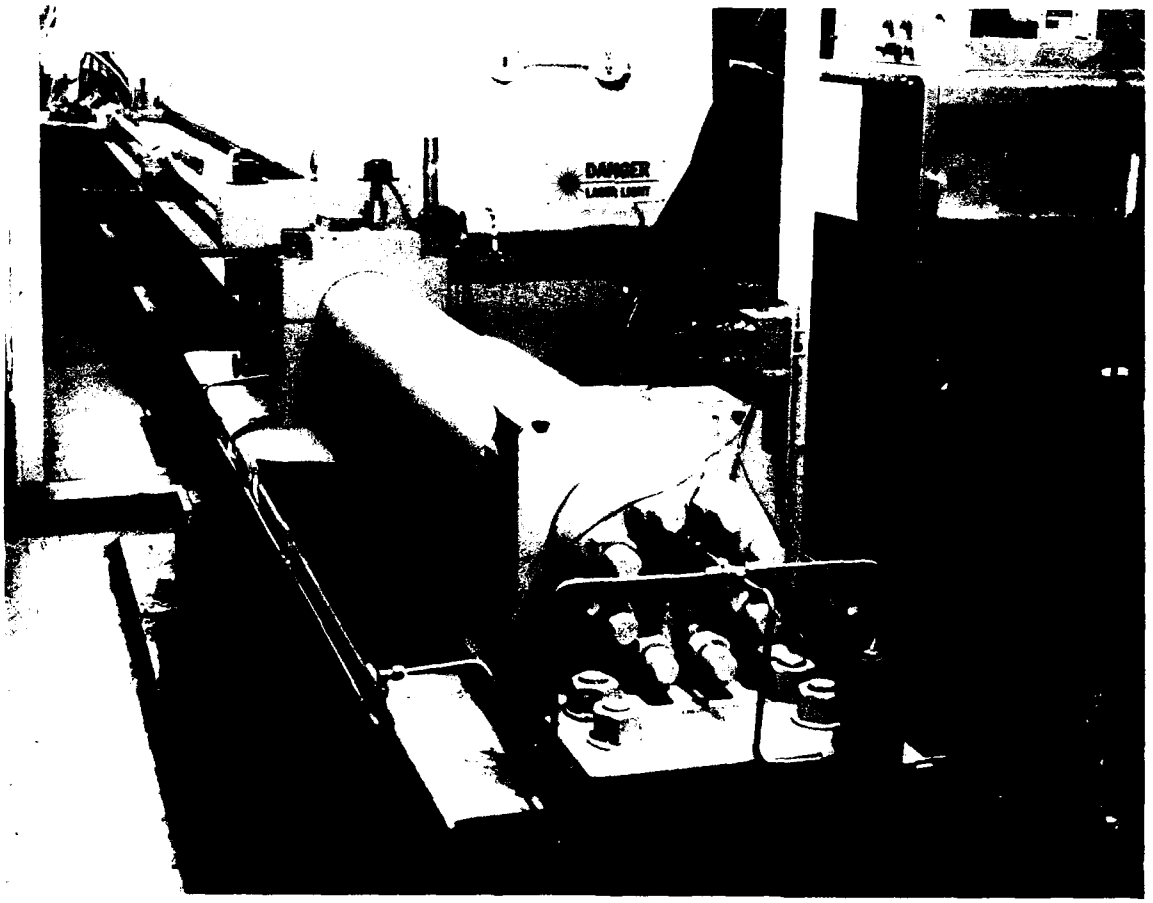

FIGURE 2. OVERVIEW OF GAS GUN FROM BREECH END

Figure 3 is a schematic of the muzzle region of the gas gun just prior to impact showing an impactor disk in a sabot and a hard steel rod supported in a frangible target holder. Electrical contact pins in the barrel wall are used to measure the sabot velocity. After impact, the sabot, impactor disk, and rod are soft recovered in a box of cloth rags. For each experiment, the disk and plug were diametrically sectioned, and a toolmaker's microscope was used to measure the plug displacement relative to the corresponding undamaged region of the impact surface of the disk.

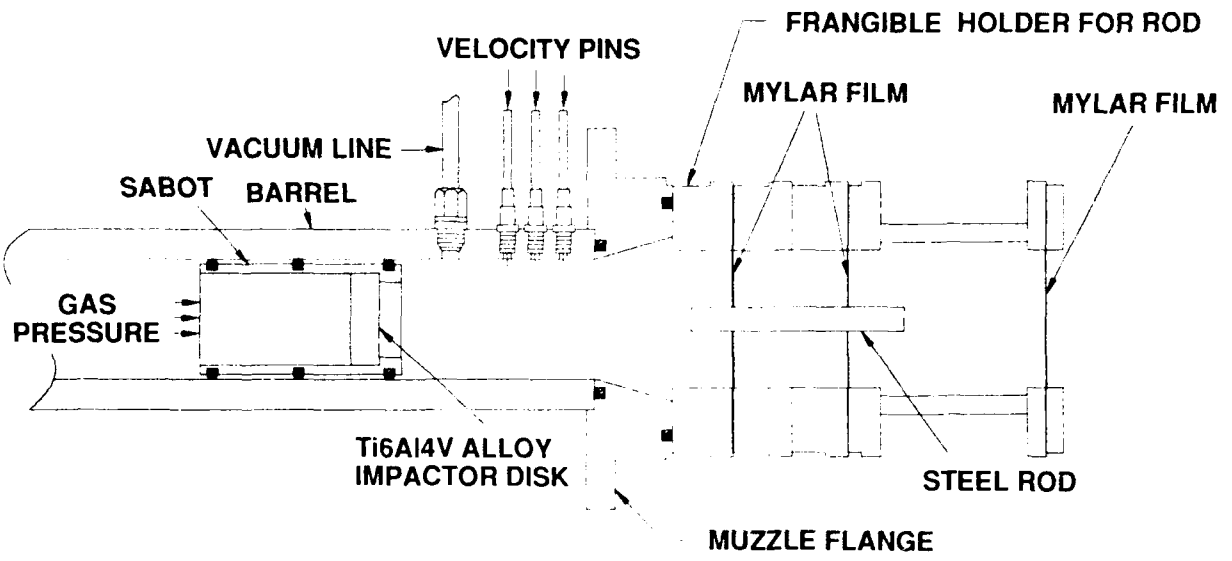

FIGURE 3. SCHEMATIC OF MUZZLE REGION OF GAS GUN

All of the impactor disks were machined from the same plate of hot-rolled and cleaned super extra-low-interstitial (super ELI) titanium alloy having a average grain size of approximately 700 microns. The vendor-supplied chemical analysis[8] indicated an oxygen content of 0.088 wt%. The disks were 9.52 mm thick and had a 34.0-mm diameter. The flat surfaces of the disks were machine-lapped with 600 grit SiC and polished with 6 micron diamond paste to minimize surface variations. The supplier's mechanical property determinations[8] give average values for 0.2 percent offset yield strength of 844.5 MPa (longitudinal to direction of plate rolling) and 833.4 Mpa (transverse to direction of plate rolling). The ultimate strength average values are 940.7 MPa (longitudinal) and 942.4 MPa (transverse). The elongation to fracture average values are 10.0 percent for both longitudinal and transverse directions. While the x-ray crystallographic determination of the texture (preferred crystallographic orientation of the grains) condition of the plate material was beyond the scope of this work, the small differences in the longitudinal and transverse mechanical properties suggest that texture effects are minimal in the original plate material.

The hardened steel rods were fabricated from dowel pins with a supplier-specified core hardness range of RC50-58.[9] The 7.94-mm diameter steel rods were machined to be 71.9 mm long, and the flat ends were polished with 6 micron diamond paste.

The range of impact velocities was from 219 m/sec to 456 m/sec. For velocities at or below 290 m/sec, the plug was pushed only partway through the disk. Figure 4 shows a rod, disk, and displaced (but not separated) shear plug. Figure 5 shows the sectioned disk and plug from the same experiment, revealing an additional shear fracture in the displaced plug. The impact velocities and corresponding plug displacements are given in Table 1.

FIGURE 4. ROD, DISK, AND DISPLACED SHEAR PLUG (283 M/SEC)

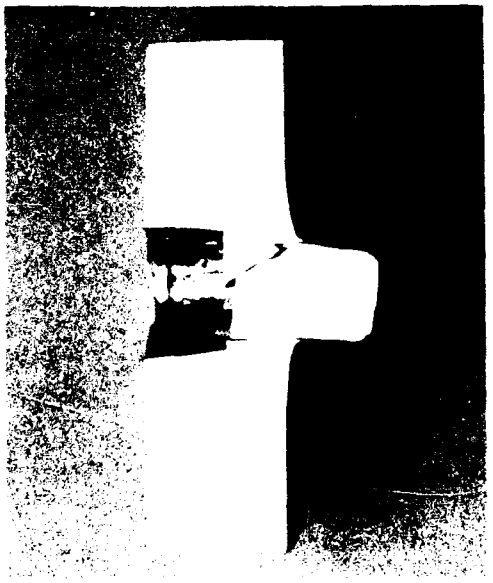

FIGURE 5. SECTIONED DISK AND SHEAR PLUG (283 M/SEC)

TABLE 1. SUMMARY OF GAS GUN IMPACT EXPERIMENTS

SHOT NUMBER	IMPACTOR VELOCITY* (M/SEC)	INITIAL IMPACT STRESS** (GPa)	INITIAL IMPACTOR THICKNESS (MM)	PLUG DISPLACEMENT (MM)
336	219	3.7	9.52	0.8
428	234	3.9	9.56	2.28
422	253	4.1	9.52	2.53
421	262	4.3	9.53	4.36
427	283	4.6	9.52	5.70
339	290	4.7	9.51	7.46
338	361	5.7	9.50	Separated from disk
337	456	7.2	9.52	Separated from disk

* Average values for two velocity intervals; the estimated uncertainty is 1 percent.

** The initial impact stress was calculated using the measured impactor velocity and calculated Hugoniot equations for these materials. The Hugoniot equations were calculated from the equation $\sigma_H = \sigma_e + \rho_e (U_S - u_e)(u_p - u_e)$ where $\rho_e = \rho_0 C_L (C_L - u_e)^{-1}$, $u_e = \sigma_e (\rho_0 C_L)^{-1}$, and $U_s = C_0 + su_p$. Here ρ_0 is the initial density, U_s is the shock velocity, C_L is the longitudinal wave velocity, σ_e is the Hugoniot elastic limit stress, and u_e is the particle velocity at the Hugoniot elastic limit. C_0 and s are the zero particle velocity intercept and the slope, respectively, of the U_s, u_p curve. σ_e was calculated from the tensile yield strength Y_0 using $\sigma_e = [(1-\nu)/(1-2\nu)]\, Y_0$, where ν is Poisson's ratio. For the Ti6Al4V alloy, the following values were used: $\rho_0 = 4.41$ Mg/m^3 (average density for seven Ti6Al4V disks), $C_L = 6.30$ km/sec,[10] $u_e = 0.101$ km/sec,[10] $\sigma_e = 2.8$ GPa,[10] and $U_s = 5.123 + 1.083\, u_p$ for $u_p < 1.4$ km/sec.[10] These values give a Ti6Al4V Hugoniot of $\sigma_H = 0.53 + 22.0\, u_p + 4.86\, u_p^2$ for $0.101 \le u_p \le 1.4$ km/sec.[10] Hugoniot data were not available for A8 steel dowel pin material. An approximate Hugoniot equation for this material was obtained from mechanical property data and the known Hugoniot of HF-1 steel.[11] For A8 steel dowel pin material, the following values were used: $\rho_0 = 7.80$ Mg/m^3 (average density for eight A8 steel dowel pins), $C_L = 5.93$ km/sec,[11] $\nu = 0.286$,[11] $U_s = 4.60 + 1.61\, u_p$,[11] and $Y_0 = 2.0$ GPa. (This 2.0-GPa tensile yield strength value is based on an assumed A8 steel hardness of RC54 and was provided by D. Goldstein of the Naval Surface Warfare Center Dahlgren Division (NSWCDD).) These values give an elastic limit stress $\sigma_e = 3.3$ GPa and an A8 steel Hugoniot of $\sigma_H = 0.75 + 34.9\, u_p + 12.7\, u_p^2$ for $u_p \ge 0.072$ km/sec.

III. MICROSCOPIC OBSERVATIONS

Figure 6 is a scanning electron micrograph (33X) of one-half of the sectioned disk from the experiment performed at 219 m/sec. showing the circular impact indentation formed by the rod end penetration. Note the raised sharp edge around the periphery of the indentation and the smooth and rough circumferential bands on the cylindrical wall. Figure 7 shows the raised edge at higher magnification (230X) with the appearance of disk material having flowed upwards very locally along the cylindrical rod surface during the indentation process. Figure 8 shows a portion of the cylindrical wall of the indentation (100X). From top to bottom in this figure, one can see first the flat impact surface of the disk and the raised edge of the indentation, then a smooth region entering the indentation, followed by a region appearing as a ductile tensile fracture surface, and finally, at the bottom, a transition region leading to an array of shear dimples. Figure 9 is an even higher magnification view (2500X) of an apparent ductile tensile fracture morphology occurring on the indentation wall. Figure 10 is a high magnification (700X) view of the shear dimples near the bottom of the indentation.

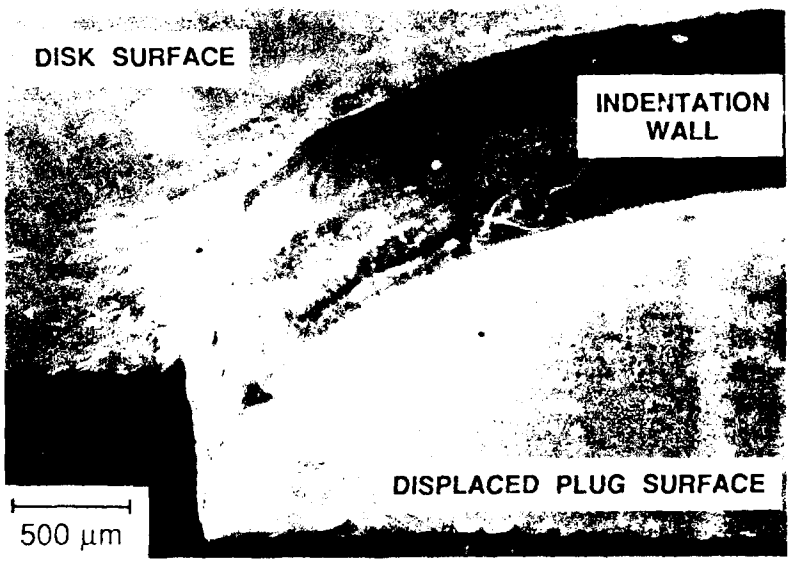

FIGURE 6. SCANNING ELECTRON MICROGRAPH OF ONE-HALF OF SECTIONED DISK (219 M/SEC) SHOWING RAISED EDGE AROUND PERIPHERY OF INDENTATION AND SMOOTH AND ROUGH EDGES ON CYLINDRICAL WALL

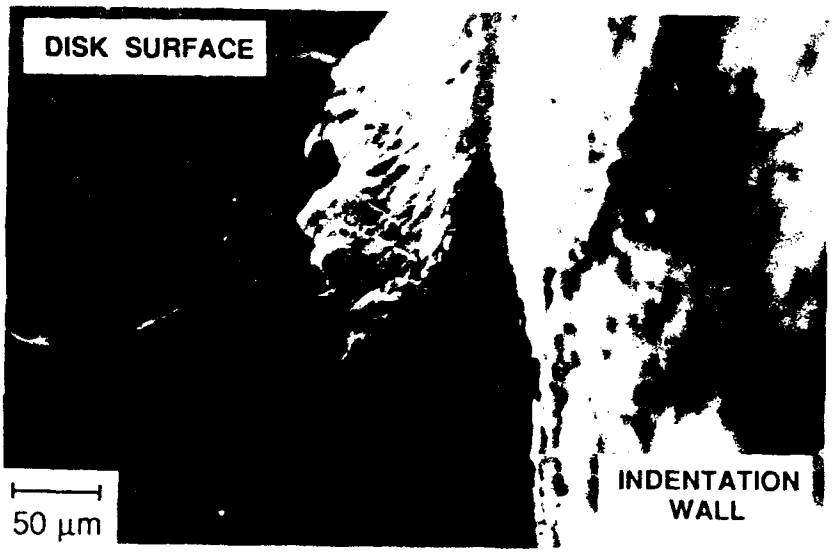

FIGURE 7. HIGHER MAGNIFICATION VIEW OF RAISED EDGE OF INDENTATION (219 M/SEC)

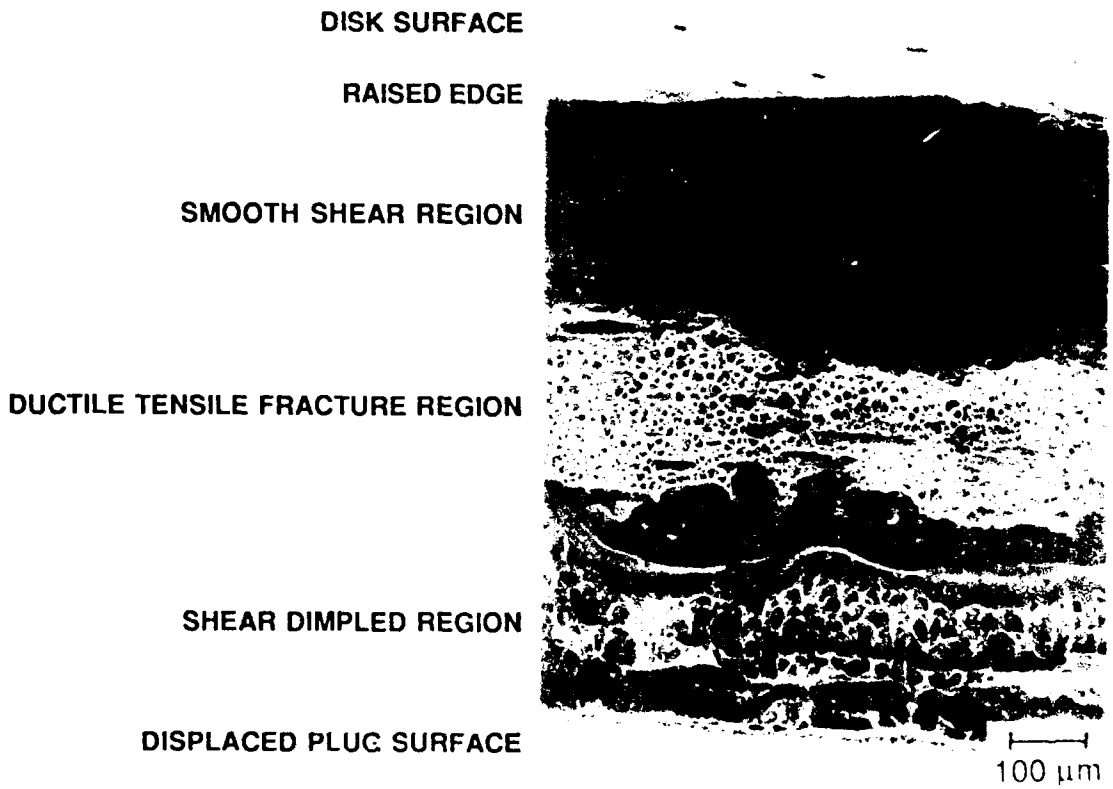

FIGURE 8. VIEW OF CYLINDRICAL WALL OF INDENTATION SHOWING VARIOUS FRACTURE MORPHOLOGY REGIONS (219 M/SEC)

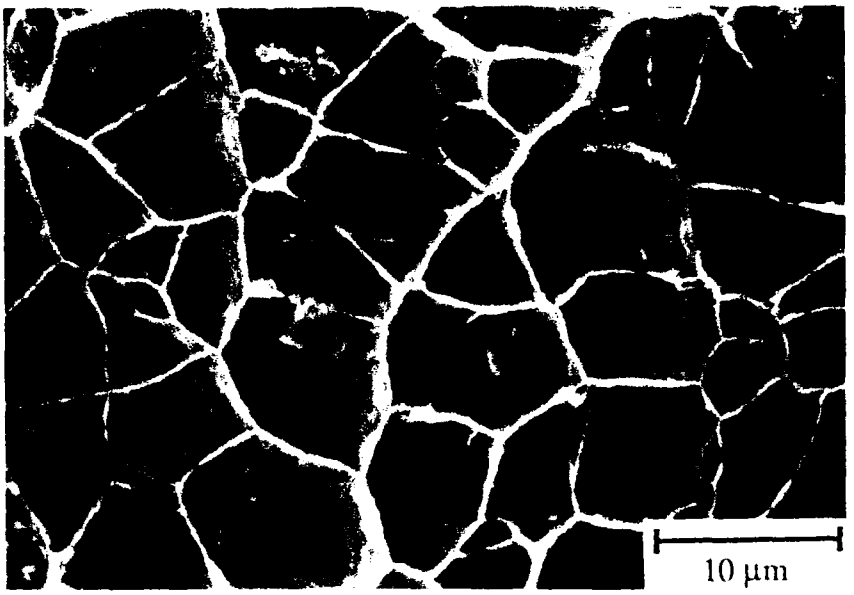

FIGURE 9. HIGHER MAGNIFICATION VIEW OF DUCTILE TENSILE FRACTURE REGION (219 M/SEC)

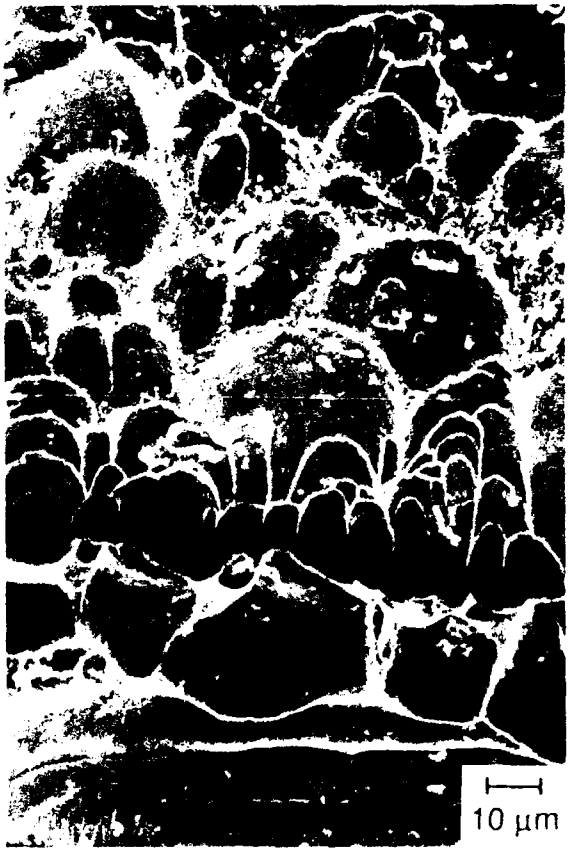

FIGURE 10. HIGHER MAGNIFICATION VIEW OF SHEAR DIMPLES NEAR BOTTOM OF INDENTATION (219 M/SEC)

An explanation for the sharp edge and smooth inner region observed near the top of the indentation is that thermally softened or even melted material has flowed out of the indentation. The radial ductile tensile fracture morphology would seem to require a bond between the titanium alloy and the steel rod that occurred where the diameter of the rod end was found to be enlarged by its own compressive deformation. As deformation-induced heating occurred at the adjacent rod/disk side wall, the higher thermal expansion coefficient for the steel relative to that for the titanium alloy should produce, on cooling, localized ductile tensile fracture of the lower strength titanium material. The appearance of shear dimples at the bottom of the indentation is consistent with the relative velocity of the disk and rod becoming zero in this region where the shear deformation has ended.

Figures 11a and b show the sectioned, polished, and etched indentation region on the other half of the disk from the 219 m/sec experiment. The rounding of corners for the indentation resulted from the electropolishing treatment. The electropolished section was etched with a 5ml HNO_3, 10 ml HF, 85 ml H_2O solution. White shear bands are seen to have nucleated near the circumference of the rod, as reported also by Woodward, et al.[12] The shear bands are observed to have cut through a relatively large, prior-equiaxed beta (bcc) grain structure that had transformed to a primary and acicular alpha (hcp) microstructure. The longest shear band (on the left in Figure 11b) is 2.4 mm in length and approximately 8 microns in width. Similar bands have been observed by Winter[13] and by Timothy and Hutchings.[14] A number of elliptical cavities of width equal to the shear band width were observed along the band lengths, as seen at the apparent grain offset in the shear band on the right of Figure 11b. Whereas the indentation depth is approximately 0.89 mm, the maximum observed displacement across the shear bands is of the order of 10 percent of the indentation depth.

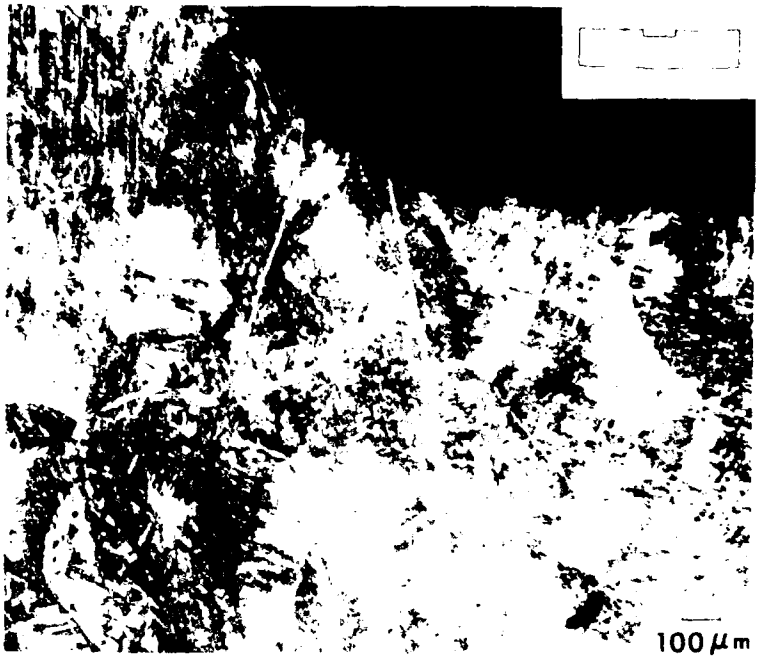

(A)

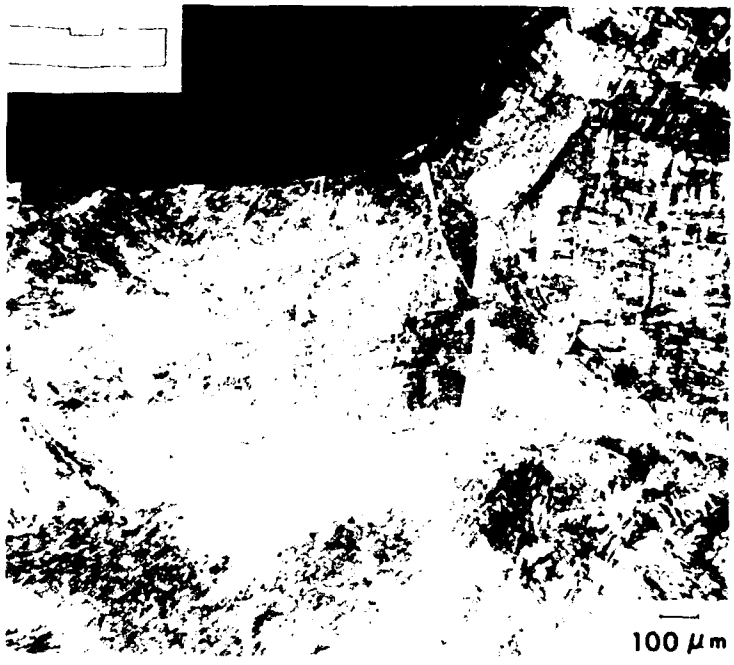

(B)

FIGURE 11. SHEAR BANDS AT INDENTATION CORNERS (219 M/SEC)

For the experiment performed at 283 m/sec, the plug was fully formed and displaced 5.70 mm, but it was not separated from the disk. Scanning electron microscopy of the shear surfaces of the plug and of the disk indentation revealed shear dimples oriented in opposite directions, which is consistent with expected relative displacement in shear.[15] Similar observations have been reported by Timothy and Hutchings.[16]

A large number of shear bands were observed in the experiment performed at 290 m/sec. In this case, a single main shear band of about 60 microns width was observed to run along the plug wall direction completely through the connected region of the plug and disk (along a length that is approximately one-quarter of the disk thickness) and also to have left a track along the exposed wall of the indentation. The observed width of this shear band is consistent with the 50-micron width calculated by Coffey[17] using a dislocation dynamics model and with the same approximate width estimated on a continuum adiabatic shear band model basis by Dodd and Bai.[18]

Figures 12 and 13 show optical and scanning electron microscope views, respectively, of the relatively thick main shear band. Except for the presence of elliptical cavities, appearing as breaks in the shear bands, the bands appeared relatively free of any finer microstructural detail. Branching into satellite bands occurred along the main shear band and for the narrower bands that spread from the main shear zone. The widths of the narrower bands were approximately equal to those shown in Figures 11a and b for the 219 m/sec experiment. The sectioned disk and plug also revealed that on the opposite side of the plug from the view of Figure 12, the plug had broken away from the disk. The fracture occurred along the main shear zone, with approximately half of the width of the white-etched region remaining with the disk and the other half with the plug.

FIGURE 12. OPTICAL MICROGRAPH OF
MAIN SHEAR BAND (290 M/SEC)

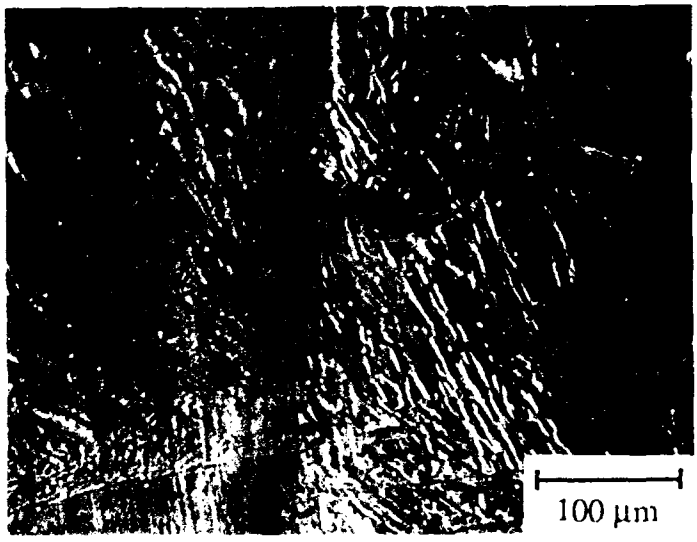

FIGURE 13. SCANNING ELECTRON MICROGRAPH OF
MAIN SHEAR BAND (290 M/SEC)

Figure 14 is a scanning electron micrograph of a central portion of the shear surface of the separated plug from the experiment at 456 m/sec. Clear evidence is observed of melted material, including a solidified metal spray thrown onto the plug, suggesting that melting had occurred just prior to plug separation. This would indicate the generation of temperatures at least as high as the 1660°C melting temperature for Ti6Al4V.[19] This melting observation is further supported by energy-dispersive-analysis of x-rays (EDAX) examination of a metallic deposit distributed over the periphery of the impact end of the steel rod, indicating the presence of titanium and aluminum, and again demonstrating that disk material was deposited on the rod. In experiments with hard steel cone-tip projectiles impacting Ti6Al4V targets, Woodward[3] has also reported evidence of melted material on the ejected shear plugs and deposits of titanium on the eroded projectile tips. Bryant, et al.[20] have observed spherical globules decorating the perimeter of dimples on shear lips in Ti10V2Fe3Al alloy deformed at a strain rate of 28 s^{-1}, supporting the view that small volumes of material in microligaments were heated above the melt temperature at final separation. Also, Ogawa and Nojima[21] have reported a decrease in strain hardening due to adiabatic heating in the compressive deformation of Ti6Al4V alloy at a strain rate of 500 s^{-1}.

FIGURE 14. SCANNING ELECTRON MICROGRAPH OF CENTRAL PORTION OF SEPARATED PLUG. THERE IS EVIDENCE OF SOLIDIFIED METAL SPRAY THROWN ONTO STRIATED SURFACE OF PLUG (456 M/SEC)

The generation of heating past the melting temperature because of adiabatic shear banding is consistent with a dislocation pileup avalanche model calculation by Armstrong, et al.[22, 23, 24] The energy stored in the pileup is liberated as heat when the pileup is catastrophically released by the collapsed obstacle. In comparison with an upper limiting temperature $\Delta T = 2.3 \times 10^5$°K given for collapse of the strongest pileup in alpha-titanium,[23] the model predicts $\Delta T = 3.6 \times 10^5$°K for the Ti6Al4V alloy; hence, a 50-percent greater heating effect is expected for the current material. A graphical analysis of this result has been reported.[25] Note that these extreme temperatures are predicted for the microscale environment in the immediate vicinity of the pileup site; after averaging over a volume containing many lattice sites in this vicinity, an observed temperature would be lower but sufficiently high for melting to occur. Calculations by Bryant, et al.,[20] on Ti10V2Fe3Al alloy suggest that the rupture of microligaments can lead to localized temperature increases of about 1840°C.

Figure 15 is a schematic drawing of the shear plugging process that summarizes the microscopic observations. On first impact of the disk with the rod, the diameter of the impact end of the rod increases somewhat via yielding in compression. Shear bands form in the stressed region of the disk, and those located along the periphery of the rod coalesce to form the boundary of the plug. As the plug begins to move, a circular array of shear dimples forms at the matching surfaces of the plug and the disk. The diameter of this array corresponds approximately to the rod diameter. As the plug is displaced farther, thermally softened, or possibly melted, disk material is extruded back along the rod to form a sharp ridge around the indentation. With additional plug displacement, material in the main shear zone melts. The consequent volume expansion on melting causes a pressure buildup that sprays molten metal onto the plug surface. The bulge behind the rod end caused by its own deformation probably contributes to reducing the flow of molten metal back along the rod length during the penetration process.

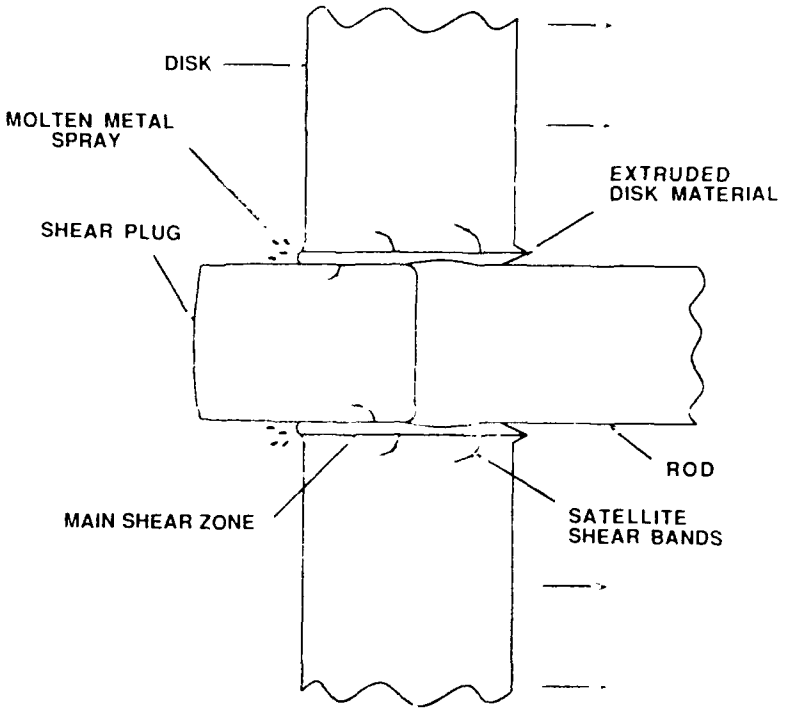

FIGURE 15. SCHEMATIC OF DISK-ROD INTERACTION

IV. MODEL FOR DISK-ROD INTERACTION

Consider a rod of diameter D and mass M_R impacting at velocity V a disk of thickness H and mass M_D. For generality, the initial velocities of the rod and disk will be taken as U and (U-V), respectively. Attention will be restricted to the case where the rod does not punch through the disk; i.e., the rod and disk move together as a single mass after impact. The velocity V_a of the rod-disk combination after impact is given by the conservation of momentum:

$$(M_R + M_D)\, V_a = M_R U + M_D (U - V)$$

or

$$V_a = U - \frac{M_D}{M_R + M_D} V \qquad (1)$$

Conservation of energy requires that the initial kinetic energy in the system equal the sum after impact of (1) the translational kinetic energy, (2) the elastic vibrational energy E_{VIB}, and (3) the plastic work done during the rod-disk interaction:

$$\frac{M_R U^2}{2} + \frac{M_D (U - V)^2}{2} = (M_R + M_D)\frac{V_a^{\,2}}{2} + E_{VIB} + \int_{x=0}^{x=h} F dx \qquad (2)$$

Here the plastic work has been expressed in terms of the relative displacement x and the force F opposing that displacement. The maximum value of x is h, which is the magnitude of penetration.

Combination of Equations 1 and 2 yields an energy balance of simple form:

$$\frac{MV^2}{2} = E_{VIB} + \int_{x=0}^{x=h} F dx \qquad \text{where} \qquad M = \frac{M_R M_D}{M_R + M_D} \qquad (3)$$

The quantity $MV^2/2$ can be thought of as the energy available in the system for altering the condition of the components. As must be the case, this energy depends only on the relative velocity of the rod and disk and not on the absolute velocities of the components or the coordinate system in which these velocities are measured.

Equation 3 makes a specific statement about the quantity of energy available, but only a general statement about its distribution. Further approximation must be applied to the terms in that equation if we are to obtain a model characterized by a few empirically determined parameters.

We begin by approximating the force F. Experiments have shown that the rod pushes from the disk a plug with a diameter approximately equal to that of the rod. The force F is assumed to arise from a constant shear stress τ acting at the interface between the plug and the disk:

$$F = \pi D (H - x) \tau \qquad (4)$$

With this linear relationship between force and displacement, the plastic work is expressed in terms of a single unknown τ

$$\int_{x=0}^{x=h} Fdx = \pi Dh\left(H - \frac{h}{2}\right)\tau \tag{5}$$

Another approximation permits the contribution of elastic vibrations to be expressed by one unknown parameter E_T. These vibrations are assumed to absorb all of the available $MV^2/2$ energy up to the threshold value E_T; for higher energies the excess goes into plastic work or plug displacement.

For the velocity range which gives $0 < h < H$, the energy balance yields for the assumptions stated an elliptical relationship between V and h:

$$\frac{MV^2}{2} = E_T + \pi Dh\left(H - \frac{h}{2}\right)\tau \tag{6}$$

Equation 6 can also be solved for h as a function of V:

$$h = H \pm \sqrt{H^2 - \frac{2}{\pi D\tau}\left(\frac{MV^2}{2} - E_T\right)} \tag{7}$$

where only the minus sign for the second term applies since $h \geq H$ corresponds to separation of the plug from the disk.

The value h=0 corresponds to the threshold condition where there is no excess energy to produce plug displacement. The threshold velocity is then:

$$V_T = \sqrt{\frac{2E_T}{M}} \tag{8}$$

At the other extreme, for h=H, the threshold velocity for plug separation is

$$V_S = \sqrt{\frac{2\left(E_T + \pi D\tau H^2\right)}{M}} \tag{9}$$

This model contains two adjustable parameters, E_T and τ, which can be chosen to provide a best fit to experimental data. Figure 16 shows a least-squares fit to Equation 7 by using data from six impact experiments. The fit provides E_T = 312 Joules and τ = 335 MPa, as well as V_T = 197 m/sec and V_S = 293 m/sec. The least-squares fit was also performed with data only from the

five experiments for which the plug was fully formed (i.e., the 219 m/sec experiment was not included) and the resulting values were E_T = 296 Joules and τ = 355 MPa, as well as V_T = 192 m/sec and V_S = 294 m/sec. The calculated shear strength can be compared to an estimated shear strength for the bulk disk material based on one-half of the average room temperature 0.2 percent offset yield strength. This gives τ_{BULK} = 420 MPa, and the fact that $\tau < \tau_{BULK}$ is consistent with the concept of thermal softening (or even melting) of the material in the shear zone.

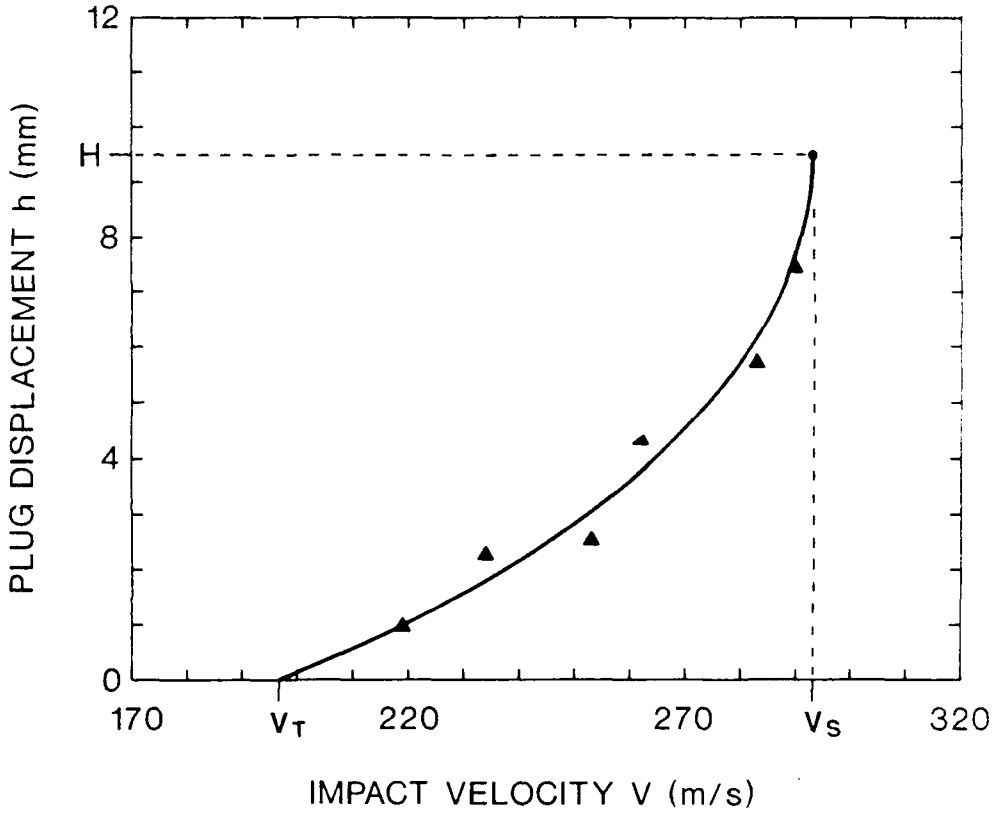

FIGURE 16. PLUG DISPLACEMENT VS. IMPACT VELOCITY. SOLID LINE IS LEAST-SQUARES FIT OF EQUATION 7 TO DATA. V_T IS THRESHOLDVELOCITY FOR PLUG SEPARATION. V_S IS THRESHOLD PLUG SEPARATION. H IS DISK THICKNESS

V. SUMMARY AND CONCLUSIONS

Reverse-ballistic impact experiments have been performed with disks of Ti6Al4V alloy and hard steel rods. Optical and scanning electron microscopies were used to probe the surfaces of the disk indentations, shear plugs of disk material, and rods to elucidate the processes of shear plug

formation and displacement. The observation of shear dimples on the plug and disk surfaces oriented in opposite directions suggest that the total punching action involves localized failure via plastic shearing. There is also evidence of thermal softening, adiabatic shear banding and melting in the sheared region. A simple model has been developed to relate shear plug displacement to impact velocity and to provide estimates of the threshold velocities for plug displacement and separation, as well as an estimate of the shear strength of the material in the main shear zone. Although microscopic observations indicate different effects in different regions of the main shear zone, including melting, the model provides an average strength for material in the zone that is less than the bulk value, consistent with thermal softening or melting.

The following conclusions[25] can be made:

1. In reverse-ballistic experiments with Ti6Al4V alloy disks impacted onto hard steel rods of smaller diameter, shear plugs were pushed out partway through the disks at impact velocities of 290 m/sec and below. At higher velocities, the plugs were completely separated from the disks.

2. For impact velocities of 234 m/sec and greater, well-defined shear bands were formed in the disks that originate from the region ot contact with the rod edges. The bands were occasionally branched and also occasionally contained cavities equal to the width of the bands.

3. The microstructure within even the widest 60-micron shear band could not be resolved up to a magnification of 4000 X with the scanning electron microscope.

4. The plug surface and the walls of any indentation/hole showed shear dimples typically oriented in opposite directions.

5. In all the experiments, a local circumferential ridge of material was extruded towards the direction of disk movement, indicating that very localized flow occurred at the earliest stages of the impacting process.

6. A spray of solidified metal thrown back onto the surface of a separated plug gave conclusive evidence of melting for high velocity impacts.

7. Plug formation has been shown to involve localized shear fracturing in addition to melting.

8. A simple model relating plug displacement to impact velocity predicts a dynamical shear strength at the disk-rod interface that is less than the conventional shear strength of the bulk material, thus giving agreement with observations that significant thermal softening has occurred in the shear zone.

9. The experimental evidence of melting prior to plug separation in this alloy is consistent with the dislocation pileup avalanche model estimates of Ti6Al4V material being even more susceptible to adiabatic heating effects than titanium material.

VI. REFERENCES

1. Timothy, S. P., *Acta Metall.*, **35**, 301, 1987.

2. Meyers, M. A. and Pak, H. R., *Acta. Metall.*, **34**, 2493, 1986.

3. Woodward, R. L., *Metall. Trans.*, **10A**, 569, 1979.

4. Me-Bar, Y. and Shechtman, D., *Mater. Sci. and Eng.*, **58**, 181, 1983.

5. Dormeval, R. and Ansart, J. P., *Journal de Physique*, Colloque C5, Supplement 8, Tome 46, 229, 1985.

6. Holt, W. H.; Mock, Jr., W.; Soper, W. G.; Coffey, C. S.; Ramachandran, V.; and Armstrong, R. W., in *Shock Compression of Condensed Matter - 1989*, Schmidt, S. C.; Johnson, J. N.; and Davison, L. W., Ed., North-Holland, 1990, p.915.

7. Mock, Jr., W. and Holt, W. H., Naval Surface Weapons Center Report NSWC TR-3473, Dahlgren, VA, 1976.

8. RMI Company, Niles, OH.

9. SPS, Inc., Jenkintown, PA.

10. Morris, C. E.; Winkler, M. A.; and Mitchell, A. C., in *Shock Waves in Condensed Matter-1987*, Schmidt, S.C. and Holmes, N.C., Eds., North-Holland, 1988, p. 265.

11. Mock, Jr., W. and Holt, W. H., *J. Appl. Phys.*, **53**, 5660, 1982. The values reported are averages for two heat treatments of HF-1 steel.

12. Woodward, R. L.; Baxter, B. J.; and Scarlett, N. V. Y., *Proc. 3rd Conf. Mech. Prop. High Rates of Strain*, Oxford, 525, 1984.

13. Winter, R. E., *Phil. Mag.*, **31**, 765, 1975.

14. Timothy, S. P., and Hutchings, I. M., *Acta Metall.*, **33**, 667, 1985.

15. Kerlins, V. "Modes of Fracture," *Metals Handbook 12*, 9th ed., ASM International, Metals Park, OH, 12, 1980.

16. Timothy, S. P. and Hutchings, I. M., *J. Mat. Sci. Lett.*, **5**, 453, 1986.

17. Coffey, C. S., *J. Appl. Phys.*, **62**, 2727, 1987.

18. Dodd, B. and Bai, Yilong, *Mater. Sci. and Tech.*, **5**, 557, 1989.

VI. REFERENCES (Continued)

19. *Metals Handbook 3*, 9th ed., ASM International, Metals Park, OH, 389, 1980.

20. Bryant, J. D.; Makel, D. D.; and Wilsdorf, H. G. F., *Mater. Sci. Eng.*, **77**, 85, 1986.

21. Ogawa, K. and Nojima, T., *Journ. Soc. Mater. Sci.*, Japan, **37**, 41, 1988.

22. Armstrong, R. W.; Coffey, C. S.; and Elban, W. L., *Acta Metall.*, **30**, 2111, 1982.

23. Armstrong, R. W. and Elban, W. L., *Mater. Sci. Eng.*, **A122**, L1, 1989.

24. Armstrong, R. W. and Elban, W. L., *Mater. Sci. Eng.*, **A111**, 35, 1989.

25. Ramachandran, V.; Zhang, X. J.; Armstrong, R. W.; Holt, W. H.; Mock, Jr., W.; Soper, W. G.; and Coffey, C. S., in *Microstructure/Property Relationships in Titanium Aluminides and Alloys*, Kim, Y. W. and Boyer, R. R., Eds., The Minerals, Metals, and Materials Society, 1991, p.647.

DISTRIBUTION

	COPIES
ATTN OP 987B MONTGOMERY COMMANDER OFFICE OF CHIEF OF NAVAL OPS NAVY DEPARTMENT WASHINGTON DC 20350-2000	1
ATTN SEA 06AR MUIR PMS 422 16 LUBIN COMMANDER NAVAL SEA SYSTEMS COMMAND WASHINGTON DC 20362-5101	1 1
ATTN A C HOLT GEORGE KOPCSAK COMMANDER OFFICE OF MUNITIONS OFFICE OF UNDERSECRETARY OF DEFENSE WASHINGTON DC 20301	1 1
ATTN OCNR213 SIEGEL COMMANDER CHIEF OF NAVAL RESEARCH OFFICE OF NAVAL TECHNOLOGY WASHINGTON DC 20350	1
ATTN DICK WILLLIAMS STEVE FISHMAN COMMANDER OFFICE OF NAVAL RESEARCH WASHINGTON DC 20360	1 1
ATTN M D ALEXANDER S A FINNEGAN N FASIG J WEEKS COMMANDER NAVAL AIR WEAPONS CENTER CHINA LAKE CA 93555-6001	1 1 1 1
ATTN E J RINEHART COMMANDER FIELD COMMAND DEFENSE NUCLEAR AGENCY FCDNA/FCTP KIRKLAND AFB NM 87117	1
ATTN C R CROWE A WILLIAMS COMMANDER NAVAL RESEARCH LABORATORY WASHINGTON DC 20350	1 1
ATTN F GRACE G E HAUVER DIRECTOR ARMY BALLISTIC RESEARCH LAB ABERDEEN PROV GRD MD 21005	1 1
ATTN L HULL W DANEN J LYMAN J REPA J M HOLT TECHNICAL LIBRARY LOS ALAMOS NATIONAL LAB LOS ALAMOS NM 87544	1 1 1 1 1 1
ATTN M J FORRESTAL CODE 9723 D E GRADY R A GRAHAM CODE 1153 TECHNICAL LIBRARY SANDIA NATIONAL LABORATORY ALBUQUERQUE NM 87115	1 1 1 1
ATTN D SHOCKEY L SEAMAN SRI INTERNATIONAL 333 RAVENSWOOD AVE MENLO PARK CA 94025	1 1

DISTRIBUTION (CONTINUED)

	COPIES
DEFENSE TECHNICAL INFORMATION CENTER CAMERON STATION ALEXANDRIA VA 22314	2
ATTN R W ARMSTRONG DEPARTMENT OF MECHANICAL ENGINEERING UNIVERSITY OF MARYLAND COLLEGE PARK MD 20742	1
ATTN S J BLESS CENTER OF ELECTROMECHANICS UNIVERSITY OF TEXAS 10100 BURNET ROAD BLDG 133 AUSTIN TX 78758	1
INTERNAL DISTRIBUTION:	
E231	3
E232	2
E281 FINK	1
E32 GIDEP	1
G06 STATON	1
G07 MOORE	1
G10	1
G13	1
G13 HOCK	1
G13 DICKINSON	1
G13 ELLINGTON	1
G20	1
G205	1
G22	1
G22 HOLT	2
G22 MOCK	2
G22 SWIERK	1
G22 SMITH	1
G22 VITTORIA	1
G22 COLLIE	1
G22 WAGGENER	1
G22 GARNETT	1
G22 CLOTFELTER	1
G30	1
G301 WILSON	1
G31 ADAMS	1
G34 FOSTER	1
H02	1
H11 MOORE	1
R04	1
R101	1
R101A REED	1
R101B HAISS	1
R11 GOTZMER	1
R13 BARDO	1
R13 COFFEY	1
R13 FORBES	1
R13 WILSON	1
R13 ZERILLI	1
R31 CLARK	1
R31 HARTMANN	1
R32 GARRETT	1
U32 MCKEOWN	1

REPORT DOCUMENTATION PAGE

Form Approved
OBM No. 0704-0188

1. AGENCY USE ONLY *(Leave blank)*	2. REPORT DATE	3. REPORT TYPE AND DATES COVERED
	June 1992	

4. TITLE AND SUBTITLE
Reverse-Ballistic Impact Study of Shear Plug Formation and Displacement in Ti6Al4V Alloy

5. FUNDING NUMBERS

6. AUTHOR(S)
William H. Holt; Willis Mock, Jr.; William G. Soper; and Charles S. Coffey

7. PERFORMING ORGANIZATION NAME(S) AND ADDRESS(ES)
Naval Surface Warfare Center Dahlgren Division (G20)
Dahlgren, Virginia 22448-5000

8. PERFORMING ORGANIZATION REPORT NUMBER
NSWCDD/TR-92/303

9. SPONSORING/MONITORING AGENCY NAME(S) AND ADDRESS(ES)

10. SPONSORING/MONITORING AGENCY REPORT NUMBER

11. SUPPLEMENTARY NOTES

12a. DISTRIBUTION/AVAILABILITY STATEMENT
Approved for public release; distribution is unlimited.

12b. DISTRIBUTION CODE

13. ABSTRACT *(Maximum 200 words)*

Gas-gun reverse-ballistic experiments have been performed in which Ti6Al4V alloy disks were impacted onto smaller diameter, hardened steel rods to push out shear plugs from the disk material. The range of disk velocities was 219 to 456 m/sec. For each experiment, the disk, plug, and rod were soft recovered after impact. Below 290 m/sec, the plugs were pushed only partway through the disks, but localized shear bands outlining the plug shapes were easily recognized in metallographic sections. Optical and scanning electron microscopies were used to determine shear zone widths and to describe microstructural details associated with the primary shear zones. There is evidence for appreciable adiabatic heating and consequent thermal softening and melting of material in the main shear zone. A simple model is used to relate the observed plug displacements to the impact velocities and to provide estimates of several features: the shear zone strength, the threshold energy for shear plug displacement, and the threshold energy for shear plug separation. Clear evidence is presented of molten material having been produced as part of the plug separation process.

14. SUBJECT TERMS
Ti6Al4V Alloy, Shear Plug Formation and Displacement, Shear Bands, Melting, Adiabatic Heating

15. NUMBER OF PAGES
33

16. PRICE CODE

17. SECURITY CLASSIFICATION OF REPORT	18. SECURITY CLASSIFICATION OF THIS PAGE	19. SECURITY CLASSIFICATION OF ABSTRACT	20. LIMITATION OF ABSTRACT
UNCLASSIFIED	UNCLASSIFIED	UNCLASSIFIED	SAR